

See discussions, stats, and author profiles for this publication at: <https://www.researchgate.net/publication/220963402>

Crowd Density Estimation Using Wireless Sensor Networks

Conference Paper · December 2011

DOI: 10.1109/MSN.2011.31 · Source: DBLP

CITATIONS

17

READS

86

4 authors, including:



Chen Qiu

Samsung Electronics America

10 PUBLICATIONS **68** CITATIONS

SEE PROFILE



Wei Xi

Xi'an Jiaotong-Liverpool University

53 PUBLICATIONS **771** CITATIONS

SEE PROFILE

Some of the authors of this publication are also working on these related projects:



xiwei@ust.hk [View project](#)

Crowd Density Estimation Using Wireless Sensor Networks

Yaoxuan Yuan, Chen Qiu, Wei Xi, Jizhong Zhao

Dept. of Computer Science and Technology, Xi'an Jiaotong University

smartyuan2009@gmail.com, chen.qiu@ymail.com, xiwei@mail.xjtu.edu.cn, zjz@mail.xjtu.edu.cn

Abstract

Estimation of crowd distribution is critical to various applications. Although most researches have provided solutions based on images and videos technologies, the high costs for deploying and an over-dependence on the bright light restrict its scope of application. In this paper, we use wireless sensor networks (WSNs) originally to make up for the lack of camera. Our approach is an iterative process which contains two phases in each time slot. In detection step, we divide the crowd density into different levels according to the RSSI data obtained by WSNs using K-means algorithm. In calibration step, we eliminate the noises and other deviations estimation based on the spatial-temporal correlation of crowd distribution. In addition, we have implemented and evaluated our algorithm by extensive real-world experiments using 16 sensor nodes and large-scale simulations. The results show that our algorithm has an accurate, efficient, and consistent performance.

Key Words - Estimation of crowd density, Wireless Sensor Networks, RSSI

I. INTRODUCTION

The ability of automatically detecting the crowd in certain environments is fundamental to various applications. The estimation of crowd density is often widely used in human safety monitoring, traffic control, smart guiding in museum and other significant applications. In order to get a precise distribution, most classical solutions are using images and video to analyze. By the steps of background modeling, changing detection, grouping and event interpretation, they can obtain the distribution of crowd density. However, these approaches are deficient in handling occlusion and crowded scenes, and the costs of complex computing also eliminate the practicability as well.

Recently, Wireless Sensor Networks (WSNs) has become an effective tool for many location-dependent services, e.g., battlefield surveillance [1], environment data collection [2][3], event or human localization [4][5], target tracking [6].

Although conventional researches have involved in many fields, the estimation for density of crowd has been seldom touched upon. Our work is originally motivated by estimating distribution of crowd density through the characteristics of WSNs. It has a high performance than camera-based mechanisms in some environments which are negatively influenced by lights. Besides, it is not necessary for special deployment to detect the density for crowds, but can reuse the WSNs which are already deployed for environment monitoring.

Although radio signal strength (RSS) is not considered as

The best choice for estimating crowd density because of unknown radio path loss factors, multi-path effects, hardware discrepancies, antenna orientation, and so forth, it does provide some useful distance related information beyond indicating connectivity among neighboring nodes. Our experimental results indicate that there is the correlation between the radio signal strength and the density of crowd, which is the fundamental assumption about our algorithm.

Relied on the empirical research, this paper introduces a mechanism for crowd density estimation using WSNs. This approach is an iterative process which has two phases in each slot: Detection and Calibration. In detection step, we receive and analysis the RSSI in our WSN environment. By K-means algorithm, the different densities of crowd in each subarea are clustered. To reduce the noises and deviation in detection phase and set a reasonable value for threshold, we design the calibration mechanism. According to spatial-temporal correlation principle, we set two assumptions to eliminate the errors. With continuous iterations, the deviation can be convergent and the result is correct.

To validate this method, an experiment with 16 wireless sensors is deployed. Experimental results demonstrate that our crowd density estimation result is accurate and acceptable. Large-scale simulations are further conducted to evaluate the scalability and efficiency. Such results are observed from intensive simulations.

The rest of the paper is organized as follows: Section 2 surveys related work. The main design is introduced in Section 3, which provides main approach to solve the problem. Section 4 reports indoor experiments and related simulations. Section 5 briefly evaluates our work by some theoretical analysis. Finally, section 6 concludes the paper.

II. RELATED WORK

There are a lot of works in the literature on crowd density estimation and monitoring. In this paper, we classify them into two categories: video-based crowd density estimation and RF-based localization.

Video-type: the traditional research works are relied on computer vision; these systems use the image from the photo devices by the steps of background modeling, changing detection, grouping and event interpretation. Head is the most prominent feature for a person in the crowd, so lots of systems estimated crowd density by using head detection method, Such as [6]. In [7] the surveillance system classified the crowd into different crowd density levels. This system was built through gray level dependence matrix method, then analyzed and estimated the group density by the crowd density levels. Davies *et al* [8] have proposed a method to esti-

mate crowd density by means of extracting two measures from the input image of the monitor areas. These two measures are the number of foreground pixels and edge pixels. The author estimated crowd density by means of the linear relationship between the number of people present in the area and the two measures. In [9], the authors used the knowledge which images of groups with different densities tend to present distinct texture patterns. A neural network and gray level dependence matrix were used.

In [10] Marana *et al.* used the Minkowski fractal dimension as a characterization of image texture firstly, the authors then described a crowd density estimation technique adopting the characterization. Kong *et al.* [11] presented a machine learning method, which used edge orientation and blob size in the image as feature for the estimation of crowd densities. In [12] the authors used an MRF-based approach, they extracted foreground firstly, and then a density estimate of the crowd was obtained through calibration information on the extracted foreground. In order to estimate the number of moving objects in a crowded scene, the authors provided a clustering technique to cluster feature points tracked across frames [13].

There are some drawbacks for most of the video-based methods of crowd density estimation mentioned above, the first is that most of them work well for scene with few and moderate people, while incapable of handling occlusion and crowded scene. The second is that most of them have a high overhead of computing, and it has a high crowd density estimation error when the environment of the scene is complicated. Using multiple cameras needs a significant amount of work and prior calibration.

RF-based localization: Some range-based localization approaches based on information such as Receive Signal Strength Indicator [14][15] are low costs, they are use RSSI to measure the distance of communication nodes. In theory, according many propagation models, RSS maps received signal strength to distance. RSSI can be obtained from many wireless communication Infrastructures which supply data service mainly. RF-based localization is a hot research issue, such as LANDMARK [16], it collected the RSSI values transmitting from the localized target objects which carry active RFID. And then, it utilized k nearest reference tags' coordinating to compute the locations of the target objects. In the paper RADAR [17], which is a radio-frequency (RF) based system for locating and tracking users inside buildings. RADAR operates by recording and processing signal strength information at multiple base stations positioned to provide overlapping coverage in the area of interest. It combines empirical measurements with signal propagation modeling to determine user location and thereby enable location aware services and applications.

In fact, RF-based localization approaches also have some disadvantages: for indoor environment, the phenomenon like reflection, refraction, diffraction caused by human bodies and other objects can eliminate the precision of Localization, such as animals, tables and so on. Temperature, humidity and the angle of antenna also can make the RSSI value changed. Hence, conventional approaches for RF-based localization are not persuasive enough.

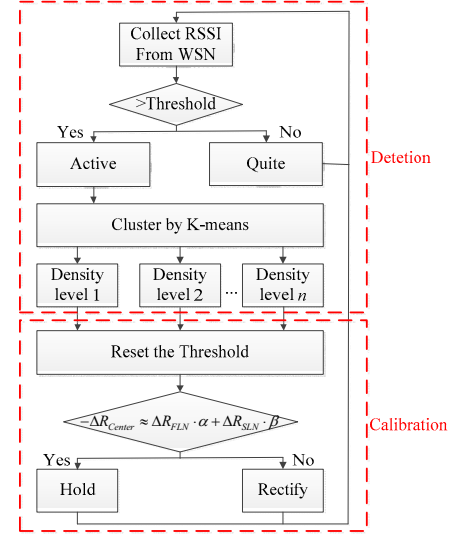


Figure 1. Overview of the estimation mechanism

III. OUR APPROACH

In this section, the details of our design are presented. We use K-means algorithm to cluster different types of crowd density. Errors are rectifying by spatial-temporal correlation in our grid network. Figure 1 describes the general diagram of our estimation algorithm. It mainly consists of two phases as follows:

Detection:

Based on the data collected from WSN, K-means algorithm clusters the several levels of density in different scenes.

Calibration:

The different areas are spatially correlated, for different slots, the whole areas are time correlated. By the two principles, rules to eliminate errors and deviations are set. Next, we will introduce the approach step by step.

For indoor environment, objects such as tables, bodies, walls and other things could obstruct the propagation of RF (Radio Frequency) signals. Some previous research works have discussed this issue. Our approach takes advantage of this effect to estimate crowd density.

Firstly, a special scene is designed to illustrate our approach. Like a museum or other proper indoor environment, it can be divided into a grid. We set a map divided by 10×10 cells. Each cell is a square region with all side 4 meters long.

To receive RSSI information, by deploying sensor nodes in the points of intersection, a special nodes distribution is organized. The WSN works on Collect Tree Protocol (CTP), which is a conventional routing protocol. All the nodes send packets to sink continuously, the packets contain the information of the RSSI values with time stamps.

A. Preliminary Experiments

To prove the feasibility of our approach, we design two simple tests in our experiment environment and draw the

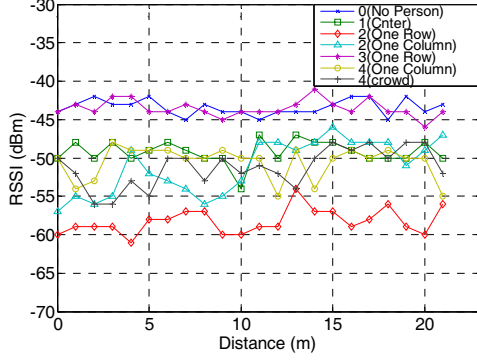


Figure 2. RSSI character for various crowd distributions

conclusion. For the first test, as Figure 2 shows, we observe the RSSI value from one WSN environment having different types of crowd distribution. Although the number of people is constant, with the changes of crowd shape, the values of RSSI are various. From this experiment, we validate that crowd distribution can express various characters through RSSI readings.

In the second experiment, the receiving RSSI by nodes reveal the following phenomenon: (1) If nobody has enter the room, the RSSI values stay in a stable level. (2) When some people join in the grid, some RSSI readings decrease immediately. (3) The more people join in the same environment, the more obviously RSSI readings change. In conclusion, the number of people has the relationship with the variation of RSSI readings in a wireless sensor network. This result can be seen in Figure 3. More people and more movements mean more changes of RSSI value. From these two kinds of experiments, we can confirm the existence of relationship between RSSI values and crowd density. This conclusion is the foundation for our further analysis.

B. Detection Algorithm

To describe our model, we introduce the time ter t_m ($t_0, t_1, t_2, \dots, t_{m-1}, t_m$) to record the slots of time.

For each cell, we need to build a database including the RSSI value for all the time of periods. This paper adopts the FingerPrint [18] algorithm to judge whether the change in a cell could be focused on. In the beginning, we record the RSSI value for each cell as the vector $C_0(c_{00}, c_{01}, c_{02}, \dots, c_{0n})$. For time slot t_m , we receive the vector $C_m(c_{m0}, c_{m1}, c_{m2}, \dots, c_{mn})$. We introduce a threshold Δ for judging. If the current RSSI values in cells exceed the threshold ($\Delta = |c_{mn} - c_{00}| > 10 \text{ dBm}$), we change their statues from 'quite' to 'active'. The 'quite' statue means the change of the cell is too little to focus on, while the 'active' statue means the change should be used for further research. In additional, how to set the value of threshold initially and change the value in each slot will be discussed in next section. For this section, to simplify the factors which are not significant, we assume that it is 10 dBm.

To obtain the distribution of whole scene, formulating acriterion to measure the density is necessary. According our

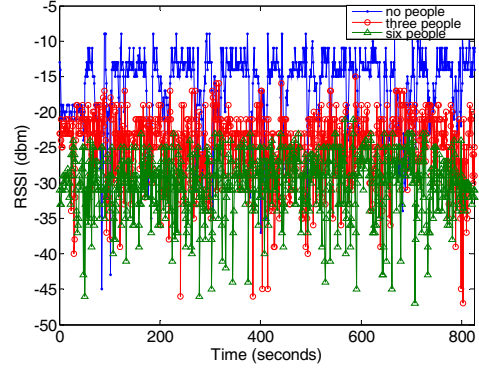


Figure 3. RSSI for different number of people

grid, we define the density of the crowd named DEN. In this paper, we use K-means clustering algorithm to classify DEN into different types. As the limitation of this paper, we just introduce K-means algorithm briefly.

The most common algorithms use an iterative refinement technique. Due to its ubiquity, it is often called the K-means algorithm [19]; it is also referred to as Lloyd's algorithm [20]. Given an initial set of k means $m_1^{(1)}, \dots, m_k^{(1)}$ (see below), the algorithm proceeds by alternating between two steps:

Assignment step: Assign each observation to the cluster with the closest mean (i.e. partition the observations according to the Voronoi[21] diagram generated by the means).

$$S_i^{(t)} = \{X_j: ||X_j - m_i^{(t)}|| \leq ||X_j - m_{i'}^{(t)}|| \text{ for all } i' = 1, \dots, k\} \quad (1)$$

Update step: Calculate the new means to be the centroid of the observations in the cluster.

$$m_i^{(t+1)} = \frac{1}{|S_i^{(t)}|} \sum_{X_j \in S_i^{(t)}} X_j \quad (2)$$

The algorithm is deemed to have converged when the assignments no longer change. What we used initialization method is Forgry [22] Partition. Forgry method randomly chooses k observations from the data set and uses these as the initial means. Forgry method tends to spread the initial means out.

To use K-means algorithm in our mechanism, we require describing the density of areas in our scene. In this paper, we design a strategy to combine the K-means algorithm and our special scene. This strategy could also be available for other scenes. As subareas of the whole grid, we could set it as a square containing 16 cells. We will count the number of active points by Fingerprint algorithm and calculate the sum of RSSI value, which are the two critical factors for classifying the density of the crowd. By statistics, the data could be listed as Table 1.

Then, iterated calculation in K-means algorithm can be processed. The subareas could be clustered for different types. As the Figure 4 showing, different density of crowd can be clustered. To the further analysis in next section, we mark the High Density as DEH, the moderate density as DEM, the low density as DEL. This criterion could be adjusted in different situations.

TABLE I. DATA FOR K-MEANS CLUSTERING

Subarea	No. of active point	Total change of RSSI value
1	2	3dbm
2	8	156dbm
...

C. Calibration

There are three key influence factors on clustering accuracy as follows:

- Noise. The noises of the indoor environment are mainly from following aspects. A) Some non-people objects could influence the RSSI value, such as animals, tables and so on. B) The communication devices like cell-phone, in radio-on state, the sending signal could Interfere RSSI. C) Other factors hard to distinguish.
- The value of threshold. As the criterion for detecting active cells, the value of threshold is critical, however, with the process of the iteration, the threshold should be adjusted to the value in each slot because of continuous environment changes. Therefore, to judge the active cell effectively, refining the value of threshold is inevitable.
- The clustering algorithm. As a classical algorithm, K-means work effectively in our experiment, but it has some error. For each circle of iteration, deviations would accumulate in period. This phenomenon will bring a negative impact.

From the above reasons, it is necessary to introduce a calibration algorithm for our mechanism, because it could provide a reasonable threshold which guaranteeing the acceptable results for iteration.

As real-time detecting system, the spatial-temporal correlation for different subareas should be underlined. On the perspective of temporal correlation, it is obviously that in a short slot of time, the variations of crowd density in certain area is limited, also, changes of RSSI value are related with the situation in former slot. For spatial correlation, the changing of density in one subarea is related with its neighbor subareas, because the crowd would move to its neighbors, or come from its neighbors in certain period. These situations can be abstracted by spatial-temporal correlation principles.

To illustrate this algorithm, a scene and several assumptions are required. This calibration algorithm would consider the subarea as the unit for researching. For a certain scene, as the description in former section, the whole area would be divided into lots of subareas. Then, according to spatial-temporal correlation, we formulate two assumptions for helping the further analysis:

- In each slot, the density of the crowd in certain subareas is stable.
- The subareas which are more close to the focused subarea have more opportunities to be influenced.

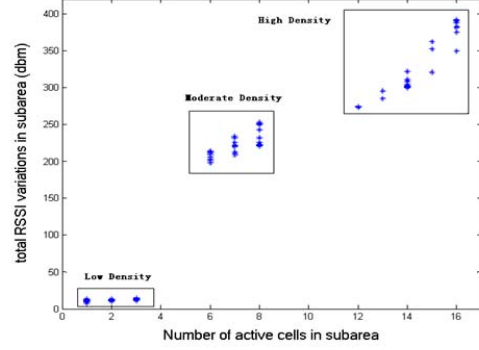


Figure 4. The result of clustering by k-means

In addition, the length of each slot is important. If length of the slot is too long, the characters about spatial-temporal correlation cannot represent obviously. If the length of the slot is too short, the costs of calculation are too much to undertake. In this paper, we set the slot of time is 1 second for our algorithm and experiment, which could make the balance between two reasons above.

As shown in Figure 5, for the center area, the inner circle of neighbors are marked as First Layer Neighbors (FLN), the external circle of neighbor are marked as Second Layer Neighbors (SLN). To simplify this question, the third even more external layers which are less correlative to focused subareas are omissible. The areas which contain FLN and SLN area are denoted as FSA. To describing the influence of these two layers, we use two coefficients to measure the influence. For FLN and SLN, the coefficients are α and β respectively.

In order to use both of the spatial and temporal correlation correctly, the threshold is needed to be calibrated in each slot. In $t_m(t_0, t_1, t_2, \dots, t_{m-1}, t_m)$, for t_m , the former time slot is t_{m-1} . The RSSI value change from t_m to t_{m-1} in each subarea could be classified. For each slot, we can calculate the value $\Delta RSSI$ by $|RSSI_{t_m} - RSSI_{t_{m-1}}|$, then, the RSSI variance in one subarea can be denoted as follows:

$$0: \Delta RSSI < 10 \text{ dBm}$$

$$1: \Delta RSSI > 10 \text{ dBm and } RSSI_{t_m} > RSSI_{t_{m-1}}$$

$$-1: \Delta RSSI > 10 \text{ dBm and } RSSI_{t_m} < RSSI_{t_{m-1}}$$

For each area which contains several subareas, it calculates the sum of the RSSI variance. For example, the variance in FLN is: $0+0+(-1)+1+1+(-1)+1+0+(-1)=0$ as shown in figure 6. It means that the RSSI change of FLN area is little. If the sum of the variance is -6, it represents the sharply decrease of density in this slot, also, If the sum of variance is 6, it represents the sharply increase of density in this slot. We denote the total variance for the area as $RV_{n_1, n_2, \dots, n_k}$ (n_1, n_2, \dots, n_k are the subareas).

As mentioned before, the threshold for iteration is the standards for choosing the active cells. To guarantee the precisely and reducing the deviation, it needs to update the threshold continuously. For each slot, the threshold Δ is the

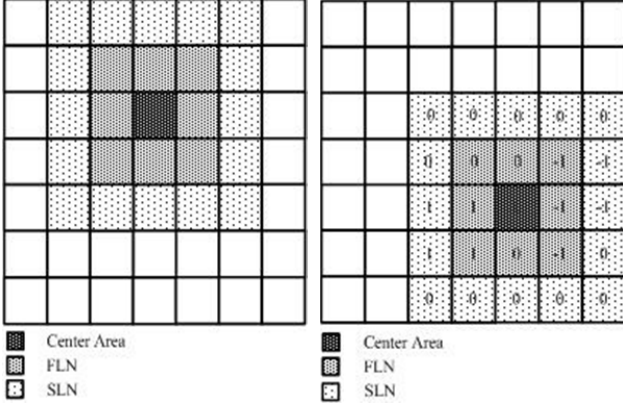


Figure 5. FLN and SLN

Figure 6. Calculation in FSA

maximum variation of RSSI marked as $MaxRV_{n_1, n_2, \dots, n_k}$. From this updating, it could choose the reasonable active cells in each subarea.

Then, the errors and deviations should be eliminated. From the time t_n to t_{n+1} , the subarea researching for can be seen as the center of FSA. The fluctuation of RSSI values can be presented by ΔR_{center} , fluctuation of RSSI values of FLN is ΔR_{FLN} , SLN is ΔR_{SLN} . As the assumptions 1 and 2, it can conclude the formula

$$|\Delta R_{center} + \Delta R_{FLN} \times \alpha + \Delta R_{SLN} \times \beta| \approx 0 \quad (3)$$

Then,

$$-\Delta R_{center} \approx \Delta R_{FLN} \times \alpha + \Delta R_{SLN} \times \beta \quad (4)$$

If the deviation between $-\Delta R_{center}$ and $-(\Delta R_{FLN} \times \alpha + \Delta R_{SLN} \times \beta)$ is beyond σ , for this slot, we would contend that the ΔR_{center} is incorrect for certain reasons, then we have to rectify the ΔR_{center} to $-(\Delta R_{FLN} \times \alpha + \Delta R_{SLN} \times \beta)$ for making the least errors (The value of σ is relied on certain situations).

In each slot of iteration, we judge and rectify results by the formula above. With times of iteration, the deviation from discussed factors could be eliminated gradually. The final result would be convergent. The related simulation and experiments refer to section 4 and 5.

IV. PERFORMANCE EVALUATION

In this section, before reporting our experimental results, we describe our experimental setup and provide the analysis of our method. Then, extension simulations are conducted to examine and evaluate the performance and effects of proposed approach.

A. Experimental setup

We carried out our experiments in an empty room (Figure 7) with 7.2×7.2 square meters. As shown in Figure 8, 16 TelosB [22] nodes were set up in a 4×4 sensor grids. All the sensors were 1.4 meters above the ground. Distance for each node was 2.4 meters except for other specified. We use 2.4 GHz ISM radio frequency band, the default transmission



Figure 7. Experiment in indoor environment

power was -10 dBm.

We connected a TelosB node to a notebook as the sink. Each node broadcasted beacon messages periodically and listened to the beacons as well. The messages contained its neighbor's RSSI values. In order to reduce beacon collisions, each node was required to wait a short random time before sending a message. We chose a beacon time interval and a RSSI message interval as 0.5, 1 second respectively. Different channels were assigned for different sensor nodes in order to avoid signal interference.

After receiving enough messages, each node reported the RSSI values for all his neighbors. This phase had to be carried out in the static environment. Then, one or more persons moved to different positions at different time intervals. Person's Moving velocity vary at $[0, 1\text{m/s}]$ randomly, also, the moving directions were random. Then we recorded the related RSSI dynamic values for all of his neighbors for a period of time, this was the dynamic environment. Then we classified crowd density for diverse levels by means of clustering method. Next, we rectified the crowd density iteratively, by the two assumptions which are relied on spatial-temporal correlation character, we use the equation (1) and (2) to judge whether it should be rectified by the parameter σ . The value of threshold was also computed and update from the iterative process.

B. Experiment Methodology

We implemented a group of experiments as our test sets. Firstly, a set of RSSI values were captured in the static environment. Then, we divided the sensor grids into 4 subareas. In different time slot, we set different persons in testing subareas respectively. Each slot repeated 10 times. In our experiments, we have tested 168 samples in the area covered by the grid at different times. In order to establish a comparison standard, the real crowd density in every subarea was manually estimated. The crowd density of the subareas was divided into different discrete levels according to the levels of crowd congestion. We set 0-3 persons in a subarea as DEL, 3-10 person in a subarea as DEM and more than 10 persons in a subarea as DEH. According to the crowd density standard, we compared the real density of the center subarea to the result from estimation approach. For our approach, we used the compared results as evaluation metric. The experiment result was presented in Figure 9.

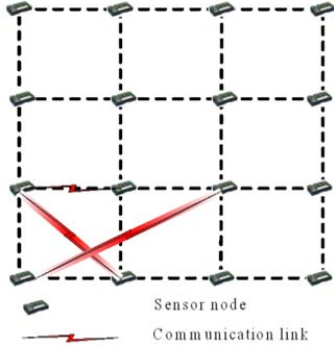


Figure 8. Test Samples

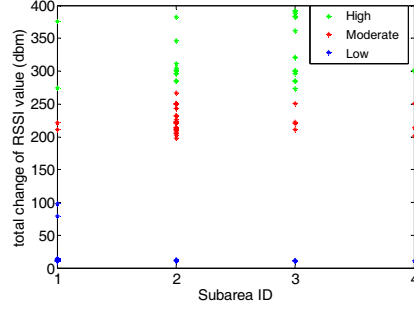


Figure 9. Three crowd density levels

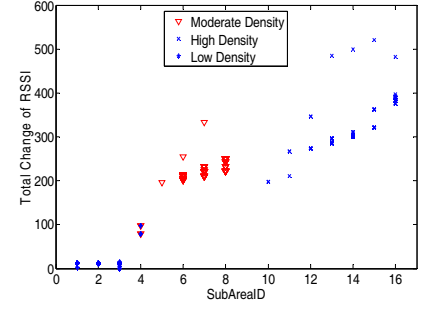


Figure 10. density estimation using more 600 samples

TABLE II. COMPARISON OF DIFFERENT FUNCTIONS IN SMAE SLOT

Density	Low(M)	Moderate(M)	High(M)
Low(E)	94%	43%	
Moderate(E)	24%	97%	19%
High(E)		14%	98%

C. Experiment Performance

In order to assess the performance of our experiment, we compare the manually estimating results to the estimative result of our tests.

Table 2 shows the comparison in one slot. The row of the table indicates the levels of density classified manually. The column of table indicates the levels of density classified by experiments. The percentages in the diagonal show the coincidence rate (named as CR) of the manual method and tests results, when the process had run for 100 times.

To analyze the influence of the movements of human bodies, the same comparison after some variations of crowd is underlined. In table 3, the results for another slot after some variations of crowd were plotted.

Different from table 2, which the results of the estimation for same levels reach a mean of 96% coincidence rate, for table 3, the changed crowd density reach a mean of 89% coincidence rate. Although the effect of estimation is worse than other estimations, the difference is not too much to be unacceptable.

In fact, the deviations of estimation are mainly attributed to the change of neighbor area density, because human movements can change the distribution of crowd density.

From the discussion above, there is a mismatch between manual estimated density and the result of our method. Because RSSI is sensitive to noise, interference, and others, the changed values of RSSI is the key point for the crowd density estimation accuracy. Besides, our crowd density estimation approach has to undergo iterative calculation processes to estimate all the subareas, it suffer significant accumulative errors. Finally, the estimation effects suffer accumulate deviations from the clustering algorithm for each circle of iteration. How to choose the appropriate parameters in our algorithm will be discussed in the discussion section.

In order to increase the performance of the approach of crowd density estimation, more training sets of RSSI variations and more levels of the density are necessary.

TABLE III. COMPARISON OF DIFFERENT FUNCTIONS IN ANOTHER SLOT

Density	Low(M)	Moderate(M)	High(M)
Low(E)	89%	43%	
Moderate(E)	31%	84%	23%
High(E)		19%	93%

D. Large-scale Simulation

Large scale simulations are further carried out to examine the scalability and efficacy of this design under varied monitoring environment. In larger scale networks environment, we designed networks of 400 nodes, deployed in a 20×20 grid, and set 5% and 10% of the data as incorrect RSSI changing values. After measuring static RSSI, people moved randomly in the region at different time, with the variation of the number of human bodies. Then, we measured and reported the related RSSI. Make use of K-means clustering and spatial-temporal correlation formulas, the results for each slot come out. For each time of evaluation, we integrated results from 300 times of iteration.

Figure 10 shows the effect of estimation for crowd density. We tested more than 600 samples for different crowd density. The result of estimation reached a mean of 81% correct estimation in despite of incorrect RSSI values. Furthermore, as figure 11 shows, when we got the convergent result, the times of iteration for our approach is less than 100 times. Because the levels of crowd density are not highly depend on the changes of RSSI values.

V. DISCUSSION

In this section, we provide the analysis of threshold value, distances for nodes, nodes transmission power and K values, which can influence the performance and efficacy of our method of crowd density estimation directly.

A. Nodes Distance

In many WSN-based monitoring systems, sensor nodes are deployed in the monitoring area randomly. They send the sensing information to the sink by multi-hops, so the node density, especially the distances between nodes are critical in our experiments. In fact, sensor nodes have limited radio range and communication radius, especially in indoor environment. Besides, signal strength is easily influenced by the

scatter wave caused by the object in the indoor room, such as building structure, persons and other goods.

There are different situations of influences for different nodes distances. For shorter distance, RSSI is strong on the Line-of-sight radio propagation, for larger node distance, RSSI is weak, because of the signal attenuation along with The distance and signal is more likely disturbed by back noises and other interferences. Clearly, the accuracy of density estimation depends on the size of the sensor grid. In certain grid, how to choose an appropriate cell size is a key issue. We conducted a test on the relationship between node distance and the variation of RSSI when the crowd density is different. After testing different distances of nodes, we verified that different nodes densities or node distances can cause different RSSI variations when crowd density distribution is varied. Some of the test results are shown in Figure 12.

We select different distances as parameters, and from the related coincidence rates and changing RSSI values. Test results show that different sensor node distances cause different RSSI threshold values. For the node distances, which are larger than 1m and smaller than 6m, the change values of the change values of RSSI are too big or too small. Among our tests, we find that the estimation effect is the best when the node distance is equal to 4m, we can observe this phenomenon from the figure 12, and we use this setting in our experiments.

B. Threshold

The threshold is critical to our solution of crowd density estimation. If the value is too high, there are no enough active points to be estimated. On the contrary, many active points caused by noise will be taken into account. For our experiment, although Δ can adjust to $MaxRV_{n_1, n_2, \dots, n_k}$, if the RSSI threshold values are lower than Δ , it is likely that the threshold values are caused by noise. Thus, we set Δ as the threshold. In each slot, the initial value of threshold also influences the coincidence rates. Also, it can decide the velocity of convergence. We test different thresholds above or below the empirical value. Based on 168 test samples, we finally find the empirical initial threshold Δ which has an ideal effect, as Figure 13 shows.

The estimate accuracy of our approach mainly depends on the RSSI threshold values. Figure 14 shows the coincidence rate in crowd density estimation at different RSSI change threshold values. In each situation the estimate accuracy increases.

C. Nodes Transmission Power

The node transmission power influences the received Signal strength, so it can eliminate the accuracy of the crowd density estimation. To observe the results of our experiments clearly, it is necessary to set the power of nodes in a proper value. In order to know how much the transmission power affects the RSSI change of two communication sensor nodes, we carried out our test use different transmission power time after time. We test 17 levels of transmission powers from -16dBm to 0dBm according to node distances ranging from 1m to 6m. As shown in Figure 15, our experiment re-

sults show that for most of the transmission power levels, the RSSI change is notable. When the node distance is short, RSSI change is not highly related with the adjustment of nodes transmission power. However, when the node distances is much longer, such as more than 5m, the RSSI change is attribute to the nodes transmission power closely. We can reduce the inter-nodal interference through reducing the transmission power. We also found that when the distance is 4m or 5m, and the transmission power is -8dBm to -11dBm, the change of RSSI has the most remarkable effect. The results for other control groups are omitted due to space limitation.

D. K Value

For the K-means clustering in our work, although the result of our approach is convergent and accurate after times of iteration, however, the choosing for initial K can also influence the convergent velocity of the process. Therefore, appropriate value for K is meaningful. As Figure 16 shows, according to our experiment, and using the threshold of -2, for comparison of values of K , when K is 2, the convergent effect of our approach is much better than other values.

VI. CONCLUSIONS AND FUTURE WORK

This paper has presented a method for crowd density estimation by analyzing the RSSI measurements in WSN. Our approach is an iteration process. For each slot, by K-means algorithm, the different densities of crowd in each grid are clustered. To make the result precisely and eliminates some deviation, we design the calibration mechanism which is according to the spatial-temporal correlation of crowd distribution. Dependent on the two assumptions, we set rules to eliminate the errors. After several iterations, the final result can be convergent.

To validate this method, a grid covered by 16 wireless sensor nodes is deployed. Large-scale simulations to further evaluate the scalability and efficiency is also implemented. Experimental results show that our crowd density estimation result is persuasive, and they are also observed from intensive simulations as well.

In general, our method maintains low cost and easy deployment, because radio can be considered as a kind of free resource. Furthermore, our method can be used in poor light that other camera-based methods of crowd density estimation cannot working or have limited effects.

In the future, we plan to try a larger monitoring area covered by the sensor nodes. The grid setting may be deployed by other topologies. Some statistical methods may be used to analyze the relationship between the change of RSSI values and the crowd motion.

ACKNOWLEDGMENT

This work is supported in part by NSFC under Grant No.60828003 and 61033015, China 973 Program under Grants No.2011CB302705.

REFERENCE

- [1] G. Simon, M. Mar'oti, 'A. L'edeczi, G. Balogh, B. Kus'y, A. N'adas et al. Sensor Network-based Countersniper System. In *SenSys'04*.

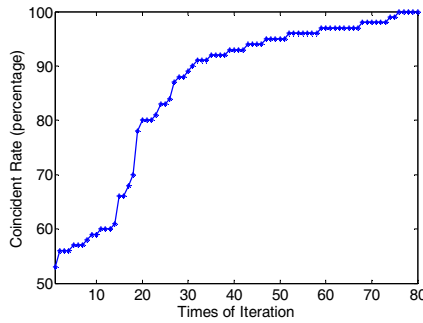


Figure 11. The convergence of large scale

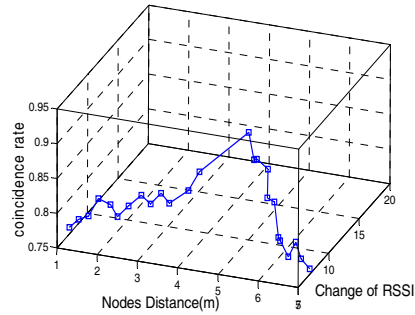


Figure 12. Different distances for different CR

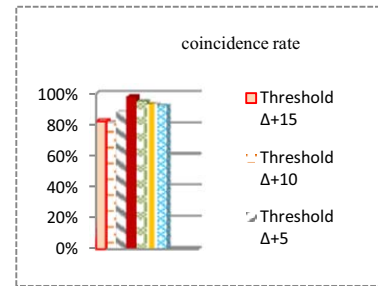


Figure 13. Tests of different threshold

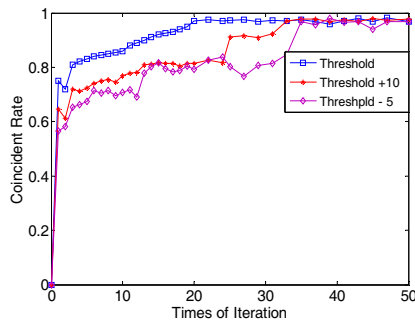


Figure 14. Convergence of our approach

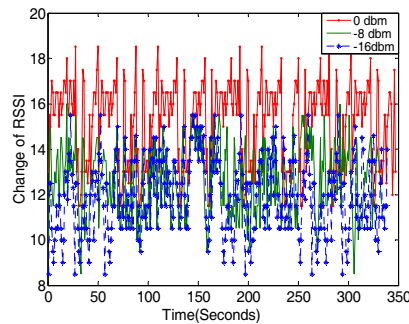


Figure 15. Final results for different power

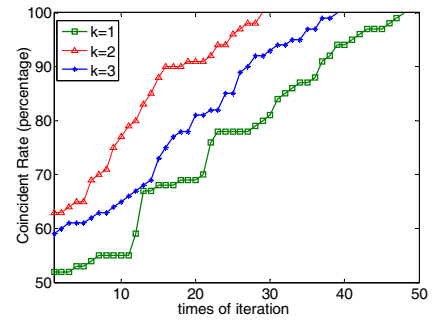


Figure 16. Final results for different K values

- [2] L. Mo, Y. He, Y. Liu, J. Zhao, S. Tang, X.-y. Li, and G. Dai, "Canopy Closure Estimates with GreenOrbs: Sustainable Sensing in the Forest," in *Proceedings of ACM SenSys*, 2009.
- [3] G. Werner-Allen, J. Johnson, M. Ruiz, J. Lees, "Monitoring Volcanic Eruptions with a Wireless Sensor Network." In *EWSN'05*.
- [4] A. Terzis, A. Anandarajah, K. Moore, I.-J. Wang, "Slip Surface Localization in Wireless Sensor Networks for Landslide Prediction." In *IPSN'06*
- [5] J. Hicks, A. Christian, B. Avery, "HPL-2005-115 Integrating Presence and Location Services using SIP." HP Labs Tech Report. June 2005.
- [6] S. McKenna, S. Gong, and Y. Raja, "Modelling Facial Colour and Identity with Gaussian Mixtures," *Pattern Recognition*, vol. 31, no. 12, pp. 1883-1892, 1998
- [7] Dian Zhang, Jian Ma, Quanbin Chen, and Lionel M. Ni. "An RF-based System for Tracking Transceiver-free Objects," In *IEEE PerCom 2007*.
- [8] R. M. Haralick, "Statistical and Structural Approaches to texture", *Proceedings of the IEEE*, vol. 67, no. 5, pp. 786-804, 1979.
- [9] A.C. Davies, J.H. Yin, S.A. Velastin, "Crowd monitoring using image processing", *Electronics and Communications Engineering Journal*, February, pp. 37-47, 1995.
- [10] Marana A N, Velastin S A, Costa L F, et al. Automatic Estimation of Crowd Density Using Texture[J]. *Safety Science*, 1998, 28 (3) :165 - 175.
- [11] A.N. Marana, L.D.F. Costa, R.A. Lotufo, S.A. Velastin, "Estimating crowd density with Minkowski fractal dimension, *Proc. IEEE Int. Conf. Acoust. Speech, Signal Process.* 6, March, 1999, 3521-3524.
- [12] D. Kong, D. Gray, H. Tao, "Counting pedestrians in crowds using viewpoint invariant training," *Proc. Br. Mach. Vis. Conf.* 2005.
- [13] N. Paragios, V. Ramesh, "A MRF-based approach for real-time subway monitoring," *Proc. IEEE Int. Conf. Comput. Vis. Pattern Recogn.* 1, 2001, 1034-1040.
- [14] V. Rabaud, S. Belongie, "Counting crowded moving objects," *Proc. IEEE Int. Conf. Comput. Vis. Pattern Recogn.* 1, June 2006.
- [15] L.M. Ni, Y. Liu, Y. C. Lau, and A. P. Patil, "LANDMARC: indoor location sensing using active RFID," in *Proceedings of the First IEEE International Conference on Pervasive Computing and Communications*, 2003.
- [16] D. Lymberopoulos, Q. Lindsey, and A. Savvides, "An Empirical Characterization of Radio Signal Strength Variability in 3-D IEEE 802.15.4 Networks Using Monopole Antennas," in *Proc. of EWSN*, 2006.
- [17] P. Bahl and V. N. Padmanabhan, "RADAR: an inbuilding RF-based user location and tracking system," in *Proceedings of the Nineteenth Annual Joint Conference of the IEEE Computer and Communications Societies*, 2000.
- [18] Otsason, V, Varshavsky, A., LaMarca, A. and de Lara, E. Accurate GSM Indoor Localization. In *Proc. UbiComp 2005*, 141-158.
- [19] J. B. MacQueen (1967): "Some Methods for classification and Analysis of Multivariate Observations, *Proceedings of 5-th Berkeley Symposium on Mathematical Statistics and Probability*", Berkeley, University of California Press, 1:281-297
- [20] P. Lloyd. Least squares quantization in pcm. *IEEE Trans. Inform. Theory*, IT-28:127-35, Mar. 1982.
- [21] M. Inaba, N. Katoh, and H. Imai. Applications of weighted voronoi diagrams and randomization to variance-based kclustering:(extended abstract). In *Proceedings of the tenth annual symposium on Computational geometry*, pages 332- 339. ACM Press, 1994.
- [22] E. Forgy, "Cluster analysis of multivariate data: Efficiency vs. interpretability of classifications", *Biometrics* 21:768. 1965.
- [23] TelosB, http://www.willow.co.uk/html/telosb_mote_platform.html.